Embedding orthogonal memories in a colloidal gel through oscillatory shear

Journal:	*Soft Matter*
Manuscript ID	SM-ART-11-2019-002222.R2
Article Type:	Paper
Date Submitted by the Author:	21-Mar-2020
Complete List of Authors:	Schwen, Eric; Cornell University, Department of Physics Ramaswamy, Meera; Cornell University, Department of Physics Cheng, Chieh-Min; Xerox Corp Jan, Linda; Xerox Corp Cohen, Itai; Cornell University, Department of Physics

SCHOLARONE™
Manuscripts

Soft Matter

ARTICLE TYPE

Embedding orthogonal memories in a colloidal gel through oscillatory shear[†]

Eric M. Schwen,[*a] Meera Ramaswamy,[a] Chieh-Min Cheng,[b] Linda Jan,[b] and Itai Cohen[a]

It has recently been shown that in a broad class of disordered systems oscillatory shear training can embed memories of specific shear protocols in relevant physical parameters such as the yield strain. These shear protocols can be used to change the physical properties of the system and memories of the protocol can later be "read" out. Here we investigate shear training memories in colloidal gels, which include an attractive interaction and network structure, and discover that such systems can support memories both along and orthogonal to the training flow direction. We use oscillatory shear protocols to set and read out the yield strain memories and confocal microscopy to analyze the rearranging gel structure throughout the shear training. We find that the gel bonds remain largely isotropic in the shear-vorticity plane throughout the training process suggesting that structures formed to support shear along the training shear plane are also able to support shear along the orthogonal plane. Orthogonal memory extends the usefulness of shear memories to more applications and should apply to many other disordered systems as well.

1 Introduction

Far from equilibrium, disordered systems can maintain memories of their preparation that can be "read out" using specific protocols.[1,2] When a memory is stored in a relevant physical parameter such as the yield strain, this memory encoding can be a useful tool for modifying the system properties. Oscillatory shear is an attractive method for embedding such memories and was first used for dilute systems of non-Brownian hard spheres.[3–5] The logic in this case is relatively clear: shearing causes the particles to bump into each other and move apart until they find a reversible state where no collisions occur during a shear cycle. Further studies have argued that this oscillatory shear memory effect should apply to disordered systems in general—shearing causes rearrangement which continues until a reversible state is found.[6–8] Indeed, similar memory effects have been found in experiments and simulations of model amorphous systems,[2,9,10] granular systems,[11] and glasses.[12–15] The interactions between particles can vary and even the nature of the "reversibility" can vary for different systems.[9,16–20] The core idea of particles rearranging and exploring possible states to find a reversible one still applies, regardless of the specifics of the system.

Colloidal gels are another interesting candidate system for memory formation since they are amorphous and have a deformable network structure that can rearrange under applied strains. Previous studies have demonstrated use of both steady and oscillatory shear for tuning the properties of a colloidal gel, finding changes in the gel structure as well as the elastic modulus.[21–28] A number of other works have described the shear history of colloidal gels from other lenses including thixotropy and accompanying structural hysteresis, where applied shear creates changes in the structure and rheology of the gel,[29–33] and soft glassy rheology (SGR) models, where time-dependent relaxations alter gel rheology.[34–40] Here, we build on these results by investigating the regime of memory formation under low-amplitude oscillatory shear to determine whether the signal of a specific applied strain can be embedded and "read out" from a gel.

2 Materials and methods

For this experiment we chose a weak colloidal gel that allowed particle rearrangement under moderate shear. The colloidal gel consisted of monodisperse, charge-stabilized silica microspheres (diameter = 1.85 μm $\pm$ 0.08 μm) suspended in an index-matched solution of glycerol and water (75-25 by mass fraction).[41] A small amount of fluorescein dye (2 mg/ml) was added to the solvent to allow imaging of the particles. Attraction was induced by the addition of magnesium sulfate salt (1M). The competition between van der Waals attraction and electrostatic repulsion creates a weak attraction between particles.[42,43] We chose particle volume fractions of $\phi \approx 35\%$ and 41% which are sufficiently high to prevent the gel from collapsing under gravity.

This gel was sheared using a custom-built biaxial shear cell with

[a] Department of Physics, Cornell University, Ithaca, NY 14850, USA. E-mail: ems445@cornell.edu
[b] Xerox Corporation, Rochester, NY 14605, USA.

a parallel plate geometry that has been described thoroughly in previous works. [44–46] The shear cell was mounted on the stage of an inverted microscope (Zeiss Axiovert 200M) with a line-scanning confocal microscopy module (Zeiss LSM 5 Live). The top plate of the shear cell is a 3 mm x 3 mm silica wafer and the bottom plate is a glass coverslip. The gap between the top and bottom plates of the shear cell was set to 30 μm. This setup allows for rapid acquisition of three-dimensional stacks of images before, during, and after applied shear. The biaxial piezoelectric controller allows investigation of nontrivial shear patterns and orthogonal readout inaccessible by standard rotational rheometry.

The colloidal gel samples were vortexed for 2 minutes and sonicated for 30 minutes before loading into the shear cell. Before each trial, the gels were subjected to a sinusoidal shear rejuvenation procedure of 200% strain applied at 20 Hz for 10000 cycles. The gels were then trained through the application of a sinusoidal strain pattern with a frequency of either 0.33 Hz or 0.50 Hz and a uniaxial strain amplitude γ_0 chosen for the specific trial. This oscillatory strain was repeated for 500-1000 cycles to allow the gels to reach steady state. Image stacks of the centers of the gels (64x64x6 μm) were taken stroboscopically (once per shear cycle) during training to analyze gel rearrangement (Fig. 1a). Stroboscopic image subtraction is our primary tool to quantify the amount of particle rearrangement between subsequent shear cycles (Fig. 1b). High levels of rearrangement show large differences between subsequent stroboscopic images, while subsequent images for a reversible state are nearly identical. Therefore, we use the average magnitude of the image difference $\langle |\Delta I| \rangle$ to quantify particle rearrangement over a single shear cycle.

We used a strain amplitude sweep to compare the gel response before and after training and assess the effect of the training procedure. For each strain sweep a selection of ~ 15 strain amplitudes γ ranging from well below to well above the training strain γ_0 were applied to the gel. Beginning from the lowest strain and proceeding linearly, five cycles at each strain amplitude were applied while imaging stroboscopically. Analyzing these images allows a measurement of the gel response at different strain amplitudes below and above the training strain.

3   Results

A core parameter controlling memory formation in disordered systems is the training strain amplitude γ_0. We trained a colloidal gel using a variety of different strain amplitudes and observed significant differences in both particle rearrangement during training and in memory readout from strain amplitude sweeps (Fig. 2).

For low strains ($\gamma_0 \approx 0.06$) the gel does not need to restructure extensively from its initial configuration and quickly reaches a reversible state. Fig. 2a shows an example of the image difference $\langle |\Delta I| \rangle$ over time where the system reaches the noise floor of our measurements early in the training process. Strain amplitude sweeps (Fig. 2b) show significantly less rearrangement in the trained gel. While the effect of training at such small amplitudes is modest, the changes observed are significantly different from those for a gel that simply ages without shear for the same period of time (Fig. S1 in ESI†).
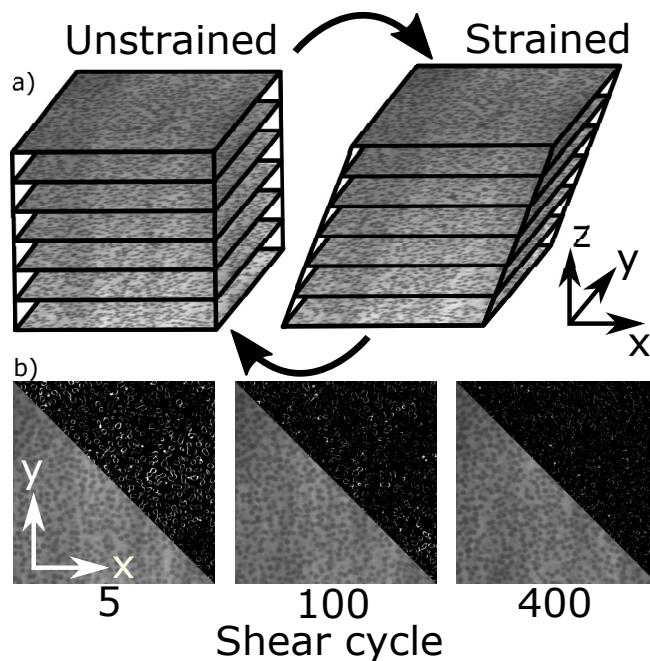

Fig. 1 Gel training procedure. (a) An oscillatory strain pattern is applied to a colloidal gel while taking 3D confocal image stacks stroboscopically. Representative slices are shown from image stacks in both unstrained and strained positions. (b) Split images show confocal images in the lower left and image difference in the upper right. Snapshots show different shear cycles during gel training. To obtain image difference, each image is filtered to remove noise and identify regions where particles are present. The later image is then subtracted from the previous cycle's image and the absolute value of this result is the image difference. High intensity areas in the image difference identify regions where a particle is present in one image but not in the other.

Moderate strains ($\gamma_0 \approx 0.19$) cause much more rearrangement and show clearer signals of both gel training and the formation of a memory of a specific training strain. The amount of rearrangement decreases with additional training cycles and approaches a reversible state with measured image difference at the noise floor (Fig. 2c). The strain amplitude sweep for the trained gel shows little to no rearrangement below the training strain—the gel can support these small strains without rearrangement (Fig. 2d). For strains larger than the training strain γ_0, the gel begins to rearrange again. The training procedure is effectively able to set a new, specific yield strain for the gel at the training strain. The training strain can be read out from the bend in the image difference data where the image difference rises above the noise floor in either Fig. 2b or Fig. 2d. This key result clearly demonstrates that our gel can form a memory of the training strain that can be read out using a strain amplitude sweep.

For higher training strains ($\gamma_0 \approx 0.21$) the gel rearrangement decreases over time but approaches a steady state image difference well above the noise floor (Fig. 2e). The gel rearranges indefinitely because the applied strain is too large to reach a reversible state. The strain amplitude sweep does show less rearrangement for the trained gel at every strain amplitude. However, the gel yields and rearranges even at low strains and the applied training strain cannot be easily read from the results (Fig. 2f).
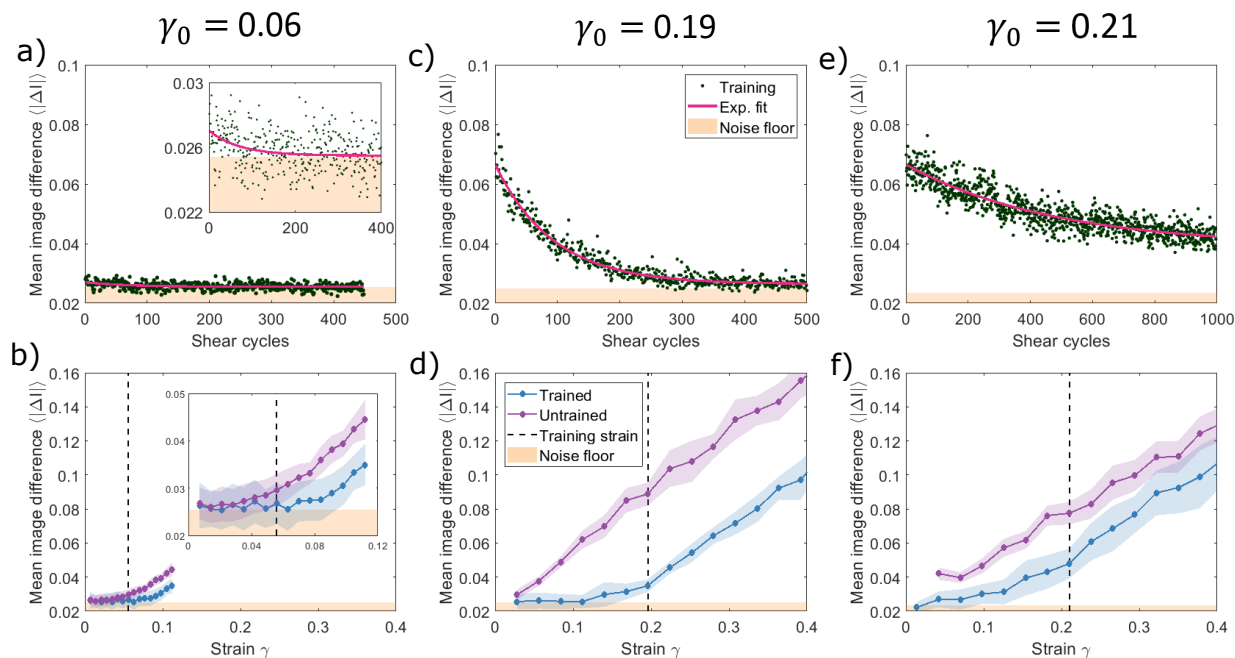
Fig. 2 Gel training results. Top row: Average magnitude of the mean image difference $\langle|\Delta I|\rangle$ during the training process as a function of shear cycles for training strain γ_0 and frequency (a) $\gamma_0 = 0.06$ at 0.5 Hz, (c) $\gamma_0 = 0.19$ at 0.33 Hz, and (e) $\gamma_0 = 0.21$ at 0.33 Hz. Pink lines show an exponential fits of the form $\langle|\Delta I|\rangle = a\exp(-t/\tau) + b$ where t is the number of shear cycles, τ is the characteristic training time, and a and b are constants. Bottom row: Strain amplitude sweeps for the gels above comparing the response of the gel to different strains before and after training. Insets show the same data with constrained axes for clarity. Results are shown for a $\phi = 35\%$ gel. Similar results are obtained for $\phi = 41\%$.

For even higher training strains, no evidence of the training is measurable. The image difference does not change throughout training and the strain amplitude sweeps show no difference between the trained and untrained gels (Fig. S1 in ESI†).

These data suggest there exists a critical training strain γ_0^c below which the gel can reach a reversible state and above which it rearranges indefinitely. Recent work[3] in memory-forming disordered systems has found power law scaling for the characteristic number of shear cycles τ required to reach a steady state following a form $\tau \sim |\gamma_0 - \gamma_0^c|^{-\nu}$ where γ_0^c is the critical strain representing the maximum effective training strain and the exponent $\nu \sim 1.3$. We do find support for this idea in our gel measurements over tens of trials using volume fractions of 35% and 41% as well as oscillatory shear frequencies of 0.33 Hz and 0.50 Hz (Fig. S2 in ESI†). However, experiments aimed at measuring the precise value of the critical strain, require long times of $\sim$ 8 hours over which we observed drift in the particle properties and the critical strain γ_0^c. We also found that γ_0^c varies between preparations. Finally, while we only report measurements where wall slip was constrained below 20% throughout the training and readout processes, this small slip can also affect measurement of the divergence at γ_0^c. Therefore experiments with even more stable systems or simulations will be needed to determine the exact value of the critical strain and power law exponent.

The different shear response between the trained and untrained gel suggests a change in the gel microstructure.[47–52] We use confocal microscopy to image the gel structure and examine how the trained gel is able to support larger strains without rearranging. We take 3D image stacks (64x64x30 μm) before and

after training as well as during pauses between shear cycles during the training process. We then locate particles using both a centroid-based method[53] and parameter extraction from reconstructing images[54] (PERI). Centroid-based methods can rapidly locate many particles in a large image volume and provide good statistics for structure measurements averaged over the system. PERI enables measurement of particle positions and radii on the nm scale and allows the precise local structure measurements. Extracting the precise particle positions and sizes allow us to use surface separation to measure nearest neighbor distributions and determine their influence on which particles are likely to rearrange.

Often, the pair distribution function provides a first measure of large structural changes in a gel. Indeed, previous studies of colloidal gels under shear have noted substantial densification of the gel[21–23,55] as a significant or even dominant factor in the rheological response of the gel. In these studies, large dense clusters and corresponding voids developed as the gel was sheared. Here, however, the lack of substantial densification is immediately apparent through visual inspection of the gel images before and after training—they are nearly indistinguishable (Fig. 1). As such, the structural modifications are significantly smaller and the pair distribution function only shows a slight increase in the primary peak (Fig. 3a).

This change in the primary peak indicates the contact number z is changing. Such contacts are important for the mechanical stability within gels and have been correlated with both gel aging[50] and the gel's ability to sustain larger strains.[24] We define particles to be in contact if their surface-to-surface separation is
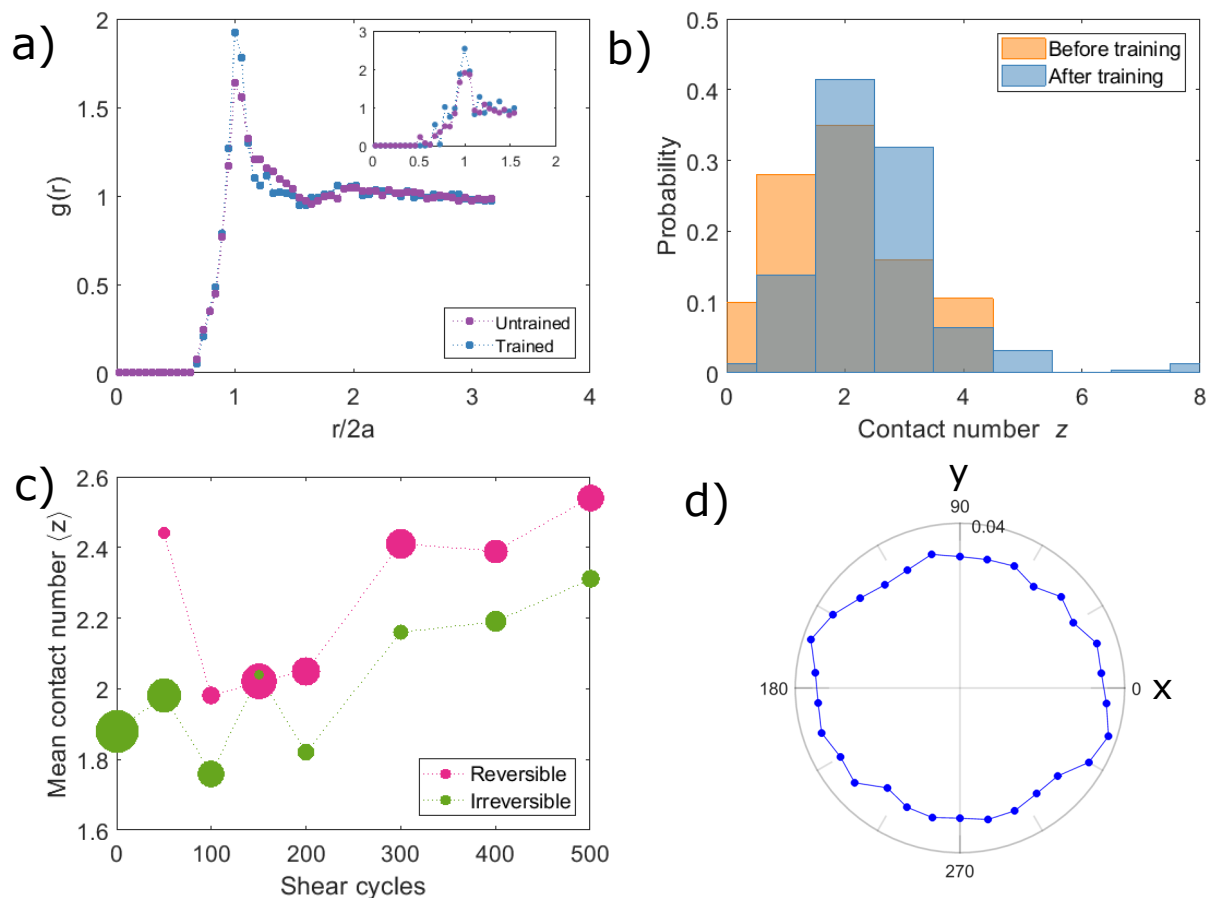
Fig. 3 Gel structure analysis. (a) Pair distribution function for a representative gel sample before and after training. Main plot uses positions from centroid-based tracking methods. Inset uses positions from PERI which is more precise but tracks fewer particles. (b) Contact number distributions for trained and untrained gel. Contacts are defined by a particle surface separation less than 50 nm as determined using PERI. (c) Mean contact number $\langle z \rangle$ plotted as a function of shear cycle for both reversible and irreversible particles. Dot size represents number of particles in the classification. (d) Bond angle probability distribution in the shear-vorticity (x-y) plane for a trained gel. Bond angles for this plot are determined for particles with center-to-center separation less than 2.1 μm. Similar results are found when bond angles are determined by surface separation (Fig. S4 in ESI†). Results are shown for a $\phi = 35\%$ gel for training strain $\gamma_0 = 0.06$ at 0.33 Hz. Similar results are obtained at other training conditions.

less than 50 nm. Using a different separation cutoff does slightly shift the mean contact number (by ~ 0.5) but does not change the observed trends. We plot the probability distributions for contact number z for a gel before and after training in Fig. 3b. After training, the gel shows a shift towards higher contact numbers.

We further analyze the data to determine how the contact number is related to particle rearrangements during training.[56,57] It is not a priori clear how these two quantities should be related. On the one hand a higher contact number indicates a more constrained environment that is less able to strain without rupture. On the other hand a network that has too low of a contact number may not be stable enough to thermal fluctuations once strained. To investigate the relationship between contact number and reversibility, we locate the particles and their neighbors as before, but now track their positions between stroboscopic images to obtain a net displacement for each particle. Using the noise floor established from an unsheared gel as a cutoff, we label any particle displacing more than 60 nm as an irreversible particle. The contact number distributions for the two populations show a signifi-

cant difference: irreversible particles tend to have fewer contacts. Put the other way, particles with fewer contacts are more likely to rearrange in a shear cycle. Plotting the mean contact number $\langle z \rangle$ at different training cycles shows that this trend of irreversible particles having fewer contacts is generally true throughout the training process (Fig. 3c). Additionally, the population of irreversible particles decreases as training proceeds and the gel approaches a reversible state. Similar results are found for the Voronoi volumes of reversible and irreversible particles (Fig. S3 in ESI†). These observations suggest a picture where irreversible particles with fewer contacts rearrange until they find a stable configuration with more contacts and join the reversible population. The end result is a trained gel with a higher contact distribution as seen in Fig. 3a.

Bond angles can also provide meaningful information about how a gel will respond to external shear. Colloidal gels under shear will sometimes arrange preferentially along the flow or vorticity axes.[23,25,29] However, measurements of our colloidal gels both before and after training show a largely isotropic distribu-
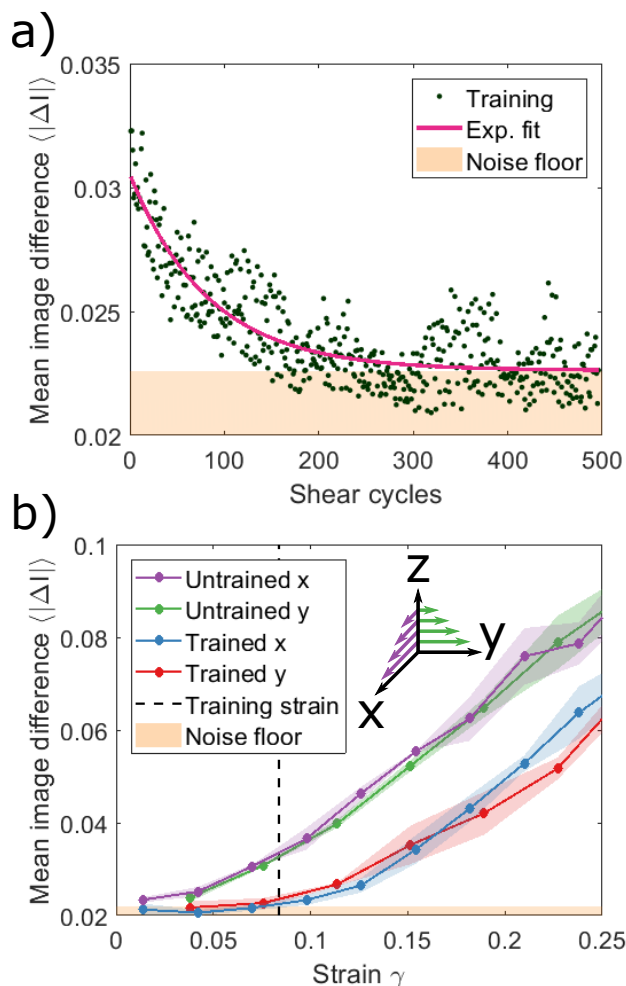
a)

b)

Fig. 4 Orthogonal training. (a) Mean image difference $\langle|\Delta I|\rangle$ as a function of shear cycles during training for training strain $\gamma_0 = 0.08$ at 0.33 Hz. (b) Strain amplitude sweeps comparing the response of the gel to along the x-z and orthogonal y-z shear planes before and after training.

tion of bond angles in the shear-vorticity plane (Fig. 3d). This lack of directionality suggests an interesting idea: if the structures formed in the trained gel also extend into the orthogonal direction, the gel may also be trained to support orthogonal shear.

In order to test the idea of orthogonal memories, we train a gel as usual by applying uniaxial shear along the x-z shear plane. For the strain amplitude sweep, however, we alternate between applying the shear along the x-z shear plane and the orthogonal y-z plane. The comparison of mean image difference before and after training shows a remarkable result—the gel is also trained to support orthogonal strains (Fig. 4). Even though the training flows were directed along the x-z plane, there is no significant difference in the trained gel response for strains applied along the x-z and y-z shear planes. This result, in combination with the even distribution of bond angles, suggests that the structures formed to support the training strain extend and support in three dimensions rather than being concentrated along the shear-gradient plane. The lack of a strong directionality also suggests that the memory effect may be robust and relevant for a variety of shear procedures that may arise in industrial use.

4 Discussion

Gels are ubiquitous in many applications ranging from beauty aids to biological gels to printer toners. The properties of a gel, however, are usually determined by the constituent materials and cannot be easily adjusted. Our measurements show that oscillatory shear training can be used to embed a memory of a specific strain in a colloidal gel. This training provides a tool to control gel properties such as the gel connectivity and yield strain without changing the materials.

The shear memories we observe bear some similarities to standard thixotropy or soft glassy rheology (SGR) approaches but demonstrate fundamental differences as well. Colloidal gels are known to be thixotropic materials where flow can induce structural changes and structural hysteresis that are both reversible and time dependent.[21,22,28,30–33,58–61] The traditional thixotropy experiment sees large changes in gel structure as applied shear breaks apart the gel into small flocs.[29] The gel reversibly reforms over time when the shear is stopped, slowly recovering its original characteristics. With our oscillatory shear training protocol, the gel instead undergoes only small, localized rearrangements and reaches a stable configuration by the time the training is done. Our training protocols are also able to set a new, higher yield strain below which the gel does not rearrange over the course of the experiment. This experimental procedure also has some similarities with descriptions of soft glassy rheology (SGR), wherein the rheology or structure of the gel changes with time.[34–40] However, the general SGR model includes a passive waiting time, while shear training memories can only be embedded by actively shearing the gel at a particular strain amplitude and frequency. Our shear training protocol establishes a threshold for induced rearrangements and sets a specific yield strain in a way that passive aging does not. In some sense, our work can be viewed as a directed aging process or a type of shear induced overaging for controlling gel properties.[62–64] Normal gel aging and may erase evidence of this training in the long term, but we did not observe significant additional aging effects over the multi-hour timescale of our observations. These distinctions, along with the evidence of a critical training strain and scaling characteristic shear cycles, show a clear phenomological difference from thixotropy and SGR models presented in previous works.

Colloidal gels provide a compelling addition to the memory effect story because they include an attractive potential between particles and a network structure. Our precision measurements of particle positions and radii[54] enabled us to show that the transition to a reversible configuration in our gels coincides with an increase in nearest-neighbor contacts at the individual particle level. Further measurements of the response of the entire network throughout a shear cycle would help identify whether the increase in contact number stabilizes the gels by increasing strand thickness or enhancing crosslinking between strands.[65–67] Other aspects of shear training memories could be addressed by adjusting the shearing frequency or gel volume fraction.[68] Both parameters are likely to change the critical training strain and the characteristic time to reach steady state. Additional studies could also relate memory formation in gels to changes in the viscoelas-

tic moduli. Previous works have linked shear-induced changes in microstructure to changing moduli.[21,22] Here, the fluid shear stresses dominate the elastic response of the weak gel so moduli changes are not easily measurable. Such changes in moduli could, however, become more dominant in denser gels.

More broadly, it would be interesting to determine whether our findings for colloidal systems extend to other systems. For example, it is possible that biological systems use oscillatory mechanisms to embed physical memories in the gels that give rise to the mechanical properties of cells and the extracellular matrix in which they reside. Rheological properties of biopolymer gels such as strain-stiffening and negative normal stresses have been linked to functions such as resisting strain injury and facilitating organelle motion.[69,70] Repetitive oscillations or shear training in biological gels could be similarly linked to facilitating operations under shear strains.

Finally, the discovery that gels can support memories in multiple shear planes despite training along a single flow direction indicates that coupling in systems that display memory may be tunable through the degree of bond isotropy. In our gel where the bonds are evenly distributed in the shear-vorticity plane, we find nearly perfect coupling of memories along different shear planes. Systems with similar isotropy, such as non-Brownian hard spheres, are expected to show similar orthogonal memory effects. In systems where such symmetries are broken, however, memories along orthogonal planes may be reduced or even eliminated providing an additional handle for tailoring the material response. Lastly, it would be interesting to consider the effect of system isotropy on memory formation in more abstract contexts. For example, in machine learning processes there are techniques for transfer learning where training a model on one task allows for solving problems in a separate but related task.[71] As we learn more about memory formation in different contexts and understand its fundamental underpinnings, this approach may emerge as a powerful method for modifying and even controlling the properties of systems both physical and abstract.

Conflicts of interest

There are no conflicts to declare.

Acknowledgements

Notes and references

1 N. C. Keim and S. R. Nagel, *Phys. Rev. Lett.*, 2011, **107**, 010603.

2 D. Fiocco, G. Foffi and S. Sastry, *Phys. Rev. Lett.*, 2014, **112**, 025702.

3 L. Corté, P. M. Chaikin, J. P. Gollub and D. J. Pine, *Nat. Phys.*, 2008, **4**, 420–424.

4 D. J. Pine, J. P. Gollub, J. F. Brady and A. M. Leshansky, *Nature*, 2005, **438**, 997–1000.

5 K. Nagasawa, K. Miyazaki and T. Kawasaki, *Soft Matter*, 2019, **15**, 7557–7566.

6 J. D. Paulsen, N. C. Keim and S. R. Nagel, *Phys. Rev. Lett.*, 2014, **113**, 068301.

7 J. P. Sethna, M. K. Bierbaum, K. A. Dahmen, C. P. Goodrich, J. R. Greer, L. X. Hayden, J. P. Kent-Dobias, E. D. Lee, D. B. Liarte, X. Ni, K. N. Quinn, A. Raju, D. Z. Rocklin, A. Shekhawat and S. Zapperi, *Annu. Rev. Mater. Res.*, 2017, **47**, 217–246.

8 N. C. Keim, J. D. Paulsen and S. R. Nagel, *Phys. Rev. E*, 2013, **88**, 032306.

9 M. Adhikari and S. Sastry, *Eur. Phys. J. E*, 2018, **41**, 105.

10 S. Farhadi and P. E. Arratia, *Soft Matter*, 2017, **13**, 4278–4284.

11 J. R. Royer and P. M. Chaikin, *PNAS*, 2015, **112**, 49–53.

12 D. Fiocco, G. Foffi and S. Sastry, *J. Phys. Condens. Matter*, 2015, **27**, 194130.

13 A. D. Parmar, S. Kumar and S. Sastry, *Phys. Rev. X*, 2019, **9**, 021018.

14 K. Hima Nagamanasa, S. Gokhale, A. K. Sood and R. Ganapathy, *Phys. Rev. E*, 2014, **89**, 062308.

15 S. Mukherji, N. Kandula, A. Sood and R. Ganapathy, *Phys. Rev. Lett.*, 2019, **122**, 158001.

16 I. Regev, C. Reichhardt and C. J. O. Reichhardt, *Modelling Simul. Mater. Sci. Eng.*, 2019, **27**, 084004.

17 J. D. Paulsen and N. C. Keim, *Proc. R. Soc. London, Ser. A*, 2019, **475**, 20180874.

18 M. Mungan and M. M. Terzi, *Ann. Henri Poincaré*, 2019, **20**, 2819–2872.

19 N. C. Keim, J. Hass, B. Kroger and D. Wieker, *arXiv*, 2018, preprint, http://arxiv.org/abs/1809.08505.

20 N. C. Keim, J. D. Paulsen, Z. Zeravcic, S. Sastry and S. R. Nagel, *Rev. Mod. Phys.*, 2019, **91**, 035002.

21 N. Koumakis, E. Moghimi, R. Besseling, W. C. K. Poon, J. F. Brady and G. Petekidis, *Soft Matter*, 2015, **11**, 4640–4648.

22 E. Moghimi, A. R. Jacob, N. Koumakis and G. Petekidis, *Soft Matter*, 2017, **13**, 2371–2383.

23 B. Rajaram and A. Mohraz, *Soft Matter*, 2010, **6**, 2246–2259.

24 L. C. Hsiao, R. S. Newman, S. C. Glotzer and M. J. Solomon, *PNAS*, 2012, **109**, 16029–16034.

25 S. Jamali, G. H. McKinley and R. C. Armstrong, *Phys. Rev. Lett.*, 2017, **118**, 048003.

26 A. P. R. Eberle, R. Castañeda-Priego, J. M. Kim and N. J. Wagner, *Langmuir*, 2012, **28**, 1866–1878.

27 M. B. Gordon, C. J. Kloxin and N. J. Wagner, *J. Rheol.*, 2016, **61**, 23–34.

28 J. C. Conrad and J. A. Lewis, *Langmuir*, 2008, **24**, 7628–7634.

29 J. Vermant and M. J. Solomon, *J. Phys. Condens. Matter*, 2005, **17**, R187–R216.

30 H. A. Barnes, *J. Nonnewton. Fluid Mech.*, 1997, **70**, 1–33.

31 J. Mewis and N. J. Wagner, *Adv. Colloid Interface Sci.*, 2009, **147**, 214–227.

32 M. T. Roberts, A. Mohraz, K. T. Christensen and J. A. Lewis, *Langmuir*, 2007, **23**, 8726–8731.

33 C. Zhu and J. E. Smay, *J. Rheol.*, 2011, **55**, 655–672.

34 G. Yin and M. J. Solomon, *J. Rheol.*, 2008, **52**, 785–800.

35 P. Sollich, F. Lequeux, P. Hébraud and M. E. Cates, *Phys. Rev. Lett.*, 1997, **78**, 2020–2023.

36 P. Sollich and M. E. Cates, *Phys. Rev. E*, 2012, **85**, 031127.

37 L. Ramos and L. Cipelletti, *Phys. Rev. Lett.*, 2001, **87**, 245503.

38 S. M. Fielding, M. E. Cates and P. Sollich, *Soft Matter*, 2009, **5**, 2378–2382.

39 D. T. Chen, Q. Wen, P. A. Janmey, J. C. Crocker and A. G. Yodh, *Annu. Rev. Condens. Matter Phys.*, 2010, **1**, 301–322.

40 H. J. Hwang, R. A. Riggleman and J. C. Crocker, *Nat. Mater.*, 2016, **15**, 1031–1036.

41 Fiber Optic Center Inc., *Angstrom Sphere Silica Particles*, http://focenter.com/wp-content/uploads/documents/AngstromSphere—-Fiber-Optic-Center-AngstromSphere-Silica-Microspheres-200um-(100g)-Fiber-Optic-Center.pdf, 2019.

42 W. B. Russel, D. A. Saville and W. R. Schowalter, *Colloidal Dispersions*, Cambridge University Press, Cambridge, England, 1989.

43 N. Eom, D. F. Parsons and V. S. J. Craig, *J. Phys. Chem. B*, 2017, **121**, 6442–6453.

44 N. Y. C. Lin, J. H. McCoy, X. Cheng, B. Leahy, J. N. Israelachvili and I. Cohen, *Rev. Sci. Instrum.*, 2014, **85**, 033905.

45 M. Ramaswamy, N. Y. Lin, B. D. Leahy, C. Ness, A. M. Fiore, J. W. Swan and I. Cohen, *Phys. Rev. X*, 2017, **7**, 041005.

46 X. Cheng, J. H. McCoy, J. N. Israelachvili and I. Cohen, *Science*, 2011, **333**, 1276–1279.

47 D. Hexner, A. J. Liu and S. R. Nagel, *Phys. Rev. E*, 2018, **97**, 063001.

48 D. Hexner, A. J. Liu and S. R. Nagel, *Soft Matter*, 2018, **14**, 312–318.

49 H. Tsurusawa, M. Leocmach, J. Russo and H. Tanaka, *Sci. Adv.*, 2019, **5**, eaav6090.

50 R. N. Zia, B. J. Landrum and W. B. Russel, *J. Rheol.*, 2014, **58**, 1121–1157.

51 B. Rajaram and A. Mohraz, *Phys. Rev. E*, 2011, **84**, 011405.

52 S. Patinet, D. Vandembroucq and M. L. Falk, *Phys. Rev. Lett.*, 2016, **117**, 045501.

53 D. B. Allan, T. A. Caswell and N. C. Keim, *Trackpy v0.2*, http://soft-matter.github.io/trackpy/v0.3.2/, 2014.

54 M. Bierbaum, B. D. Leahy, A. A. Alemi, I. Cohen and J. P. Sethna, *Phys. Rev. X*, 2017, **7**, 041007.

55 H. K. Chan and A. Mohraz, *Phys. Rev. E*, 2012, **85**, 041403.

56 J. M. van Doorn, J. Bronkhorst, R. Higler, T. van de Laar and J. Sprakel, *Phys. Rev. Lett.*, 2017, **118**, 188001.

57 C. J. Dibble, M. Kogan and M. J. Solomon, *Phys. Rev. E*, 2008, **77**, 050401.

58 J. Mewis, A. J. B. Spaull and J. Helsen, *Nature*, 1975, **253**, 618–619.

59 J. Vermant, *Curr. Opin. Colloid In.*, 2001, **6**, 489–495.

60 E. Moghimi, A. R. Jacob and G. Petekidis, *Soft Matter*, 2017, **13**, 7824–7833.

61 L. C. Johnson, R. N. Zia, E. Moghimi and G. Petekidis, *J. Rheol.*, 2019, **63**, 583–608.

62 V. Viasnoff and F. Lequeux, *Phys. Rev. Lett.*, 2002, **89**, 065701.

63 D. J. Lacks and M. J. Osborne, *Phys. Rev. Lett.*, 2004, **93**, 255501.

64 N. Pashine, D. Hexner, A. J. Liu and S. R. Nagel, *Sci. Adv.*, 2019, **5**, eaax4215.

65 L. C. Johnson, B. J. Landrum and R. N. Zia, *Soft Matter*, 2018, **14**, 5048–5068.

66 J. Colombo and E. Del Gado, *J. Rheol.*, 2014, **58**, 1089–1116.

67 J. M. van Doorn, J. E. Verweij, J. Sprakel and J. van der Gucht, *Phys. Rev. Lett.*, 2018, **120**, 208005.

68 P. A. Smith, G. Petekidis, S. U. Egelhaaf and W. C. K. Poon, *Phys. Rev. E*, 2007, **76**, 041402.

69 P. A. Janmey, M. E. McCormick, S. Rammensee, J. L. Leight, P. C. Georges and F. C. MacKintosh, *Nat. Mater.*, 2007, **6**, 48–51.

70 C. Storm, J. J. Pastore, F. C. MacKintosh, T. C. Lubensky and P. A. Janmey, *Nature*, 2005, **435**, 191–194.

71 Y. Bengio, A. Courville and P. Vincent, *IEEE Trans. Pattern Anal. Mach. Intell.*, 2013, **35**, 1798–1828.